Energy-Aware Spiral Coverage Path Planning for UAV Photogrammetric Applications

Tauã M. Cabreira, Carmelo Di Franco, Paulo R. Ferreira Jr., and Giorgio C. Buttazzo

***Abstract*—Most unmanned aerial vehicles nowadays engage in coverage missions using simple patterns, such as back-and-forth and spiral. However, there is no general agreement about which one is more appropriate. This letter proposes an E-Spiral algorithm for accurate photogrammetry that considers the camera sensor and the flight altitude to apply the overlapping necessary to guarantee the mission success. The algorithm uses an energy model to set different optimal speeds for straight segments of the path, reducing the energy consumption. We also propose an improvement for the energy model to predict the overall energy of the paths. We compare E-Spiral and E-BF algorithms in simulations over more than 3500 polygonal areas with different characteristics, such as vertices, irregularity, and size. Results showed that E-Spiral outperforms E-BF in all the cases, providing an effective energy saving even in the worst scenario with a percentage improvement of 10.37% up to the best case with 16.1% of improvement. Real flights performed with a quadrotor state the effectiveness of the E-Spiral over E-BF in two areas, presenting an improvement of 9% in the time and 7.7% in the energy. The improved energy model increases the time and the energy estimation precision of 13.24% and 13.41%, respectively.**

***Index Terms*—Aerial systems: Applications, autonomous vehicle navigation, coverage path planning, energy-aware approach, unmanned aerial vehicles.**

I. Introduction

THE unmanned aerial vehicles (UAVs) have been used in several application domains, such as photogrammetry [1], search and rescue missions [2], crop field monitoring [3], forest fire surveillance [4], ice management information gathering [5], landmines detection [6], power lines inspection [7], and photovoltaic plant planning and monitoring [8]. Many of these UAVs applications are related to the Coverage Path Planning (CPP) problem, which is a subtopic of robot motion planning and consists of determining a path that guarantees that an agent will pass over every point in a given environment [9].

Manuscript received February 24, 2018; accepted June 20, 2018. Date of publication July 16, 2018; date of current version August 2, 2018. This letter was recommended for publication by Associate Editor E. Johnson and Editor J. Roberts upon evaluation of the reviewers' comments. The work of T. M. Cabreira was supported in part by CAPES under Grant 88881.136005/2016-01. The work of P. R. Ferreira Jr. was supported in part by CNPq under Grant 308487/2017-6. *(Corresponding author: Tauã M. Cabreira.)*

T. M. Cabreira and P. R. Ferreira Jr., are with the Programa de Pós-Graduação em Computação, Universidade Federal de Pelotas, Pelotas 96040000, Brazil (e-mail: tmcabreira@inf.ufpel.edu.br; paulo.ferreira@inf.ufpel.edu.br).

C. D. Franco and G. C. Buttazzo are with the ReTiS Laboratory, TeCIP Institute, Scuola Superiore Sant'Anna, Pisa 56124, Italy (e-mail: c.difranco@santannapisa.it; g.buttazzo@santannapisa.it).

Digital Object Identifier 10.1109/LRA.2018.2854967

Most UAVs nowadays engage in missions based on CPP using simple geometric flight patterns [10]. The one that is employed the most in real-world scenarios is the back-and-forth (BF), also known as zigzag move or lawnmower pattern. Following the BF, the UAV executes long straight movements and 180° turning maneuvers when it reaches the border of the area. The most popular flight-control software [11] implements this approach to allow flights based on an offline programmed plan. Following the same idea, one can design a spiral flight pattern (SP) where the UAV flies in circles, slowly decreasing the circle radius while flying towards the center. Both flight patterns deal with the problem requiring very low computation and no communication [12].

Despite the extensive use of these flight patterns, there is no general agreement about which one is more appropriate. Some studies highlight that the BF pattern is better [12], while other works claim that the SP pattern overcomes the BF [10], depending on the adopted criteria. Furthermore, usually the patterns are evaluated using the number of turns as the main performance metric [13], [14]. However, when dealing with UAVs on CPP missions, the number of turns is not an accurate metric for different flight patterns and several additional aspects must be considered, such as the vehicle dynamics, the distance traveled, and the optimal speed adopted during the path. These aspects directly affect the energy consumption of UAVs during the missions, especially in quadrotors whose flight autonomy is limited. Moreover, it is important to highlight that, in literature, it is still missing an energy-aware spiral pattern with accurate overlapping for photogrammetric applications using different speeds to optimize and save energy.

This letter proposes a novel Energy-aware Spiral Coverage Path Planning algorithm (E-Spiral) especially designed for photogrammetry. The algorithm considers the camera characteristics as image resolution and field of view, avoids traveling over already visited zones and applies the overlapping rates necessary to build a mosaic - commonly used in this type of application. The algorithm also uses different optimal speeds for each straight segment of the path, according to the energy model proposed in [1].

As a further contribution, the energy cost of the spiral path is estimated through an improved version of the energy model proposed in [1]. Several flights were performed at different speeds in order to analyze the behavior of the spiral pattern regarding the acceleration/deceleration phases during the turning maneuvers. Finally, the proposed approach has been compared with the E-BF, an energy-aware back-and-forth algorithm described

in [1], through a wide range of simulations on over more than 3500 polygonal areas of interest with different characteristics, such as the number of vertices, the irregularity, and the size of the area. Real flights were also performed with a quadrotor with both algorithms in two different scenarios in order to validate the proposed approach and compare the energy spent during the missions with the one estimated by the energy model. Results showed that E-Spiral outperforms E-BF in all the cases, providing an effective energy saving even in the worst scenario (large areas and few vertices) with a percentage improvement of 10.37% up to the best case (high number of vertices) with 16.1% of improvement.

The remainder of this paper is organized as follows: in Section II, it is discussed the related work regarding the spiral and back-and-forth patterns. Section III presents the E-Spiral, an algorithm aiming at optimizing the overlapping and the energy consumption. Section IV shows the experiments performed in order to improve the energy model proposed in [1] to correctly estimate the energy consumption during the spiral paths. Section V discusses the comparison between the E-Spiral and the E-BF approaches through a set of experiments performed on MATLAB simulations and on a real system; and finally, Section VI draws conclusions and future work.

II. Related Work

Several studies in the literature focus on the coverage path planning autonomy, exploring different flight patterns to perform mapping missions in a certain area. Among them, in [10], five types of flight patterns from the *US National Search and Rescue Manual* are analyzed for missions in rectangular areas, including two variations of back-and-forth (parallel and creeping line), spiral (also known as square), sector search and barrier patrol. According to the simulation results, [10] point out that the spiral pattern presents the best performance in metrics as target detection and area coverage. However, the author was not able to validate the simulation results due to problems occurred during the real flights performed at an airport - even considering a small scale practical experiment with a restricted search area and a reduced flight duration of around five minutes. Besides that, the flight tests were conducted without the extra payload of an on-board camera.

The back-and-forth and spiral patterns in concave and convex polygonal areas are explored in [12]. The authors combine the two patterns with different area decomposition techniques and conclude that the back-and-forth approach without area decomposition presents good and trustworthy results in relation to the other variations. According to them, the reliability lies in the fact that all the turning maneuvers have 90°, making the UAV behavior predictable after four maneuvers. However, the spiral pattern generates shorter paths in rounded-shape areas with large inner angles. In some complex shapes, the algorithm may finish its run without entirely covering the area. Hybrid variations with area decomposition usually create smaller paths, but the algorithms never handle all the cases in a satisfactory way.

An exact cellular decomposition method for CPP in concave polygons is presented in [13]. The area of interest is decomposed into convex subregions using a minimum width sum algorithm based on the greedy recursive method [15]. An optimal line sweep direction can be obtained by drawing a line for each edge to the most distant vertex of the polygon (Euclidean distance) in the convex subregions. Once the minor line is found, back-and-forth movements perpendicular to this line can be performed minimizing the number of turning maneuvers. Different sweep directions for each convex subregion are employed to achieve an optimal result in concave polygons. Finally, the combination of subregions is converted to the minimum traversal of undirected graph to connect the coverage path of the subregions.

A coverage path planning approach in convex and non-convex areas for the acquisition of aerial images for 3D reconstruction is proposed in [14]. A back-and-forth pattern perpendicular to the optimal line sweep direction is used to cover convex polygons. In concave shapes it is necessary to verify if the coverage can be done using the pattern with no interruptions in the stripes. If there is an interruption, an exact decomposition is employed to generate concave and convex subregions. The authors also explore four alternatives of back-and-forth movements regarding the direction and the orientation of the movement, trying to minimize the transition distance between the subregions in order to minimize the path total length. Finally, the authors consider a closed coverage path, where the endpoint connects to the starting point through a straight line.

The previously mentioned studies usually consider the minimization of the number of turning maneuvers in order to reduce the execution time and the energy consumption of the mission. Performing several turns leads to a considerable amount of time and energy spent due to the deceleration/acceleration process. In [1], an energy-aware back-and-forth approach has been proposed using an energy model derived from real measurements. The optimal speed is set at each straight segment of the path considering the traveled distance for reducing the total energy consumption. Despite the energy saving in the straight parts, this pattern still presents 90° turns where the speed of the UAV drastically decreases in every maneuver.

In a spiral pattern, the deceleration of the UAV at each turn directly depends on the angle necessary to perform the maneuver. In areas with larger inner angles, it is possible to perform smoother turns, saving time and energy. Furthermore, to the best of our knowledge, a spiral pattern for photogrammetry considering accurate overlapping is missing in the literature. Thus, it is proposed an energy-aware spiral coverage path planning algorithm with optimal speed, smooth turning maneuvers, and proper overlapping to guarantee the mission success.

The effect of wind fields in the path planning involving fixed-wings vehicles is explored in [16], [17]. Energy-efficient trajectories can be planned using the optimal speed that minimizes the energy consumption considering an energy map built over a complex wind field. However, the authors are not considering missions to cover an entire area. Instead, they are exploring missions consisting of traveling from one point to another or passing by a small set of points. We intend to explore the effect of winds in a near future for coverage missions after validating the proposed approach.

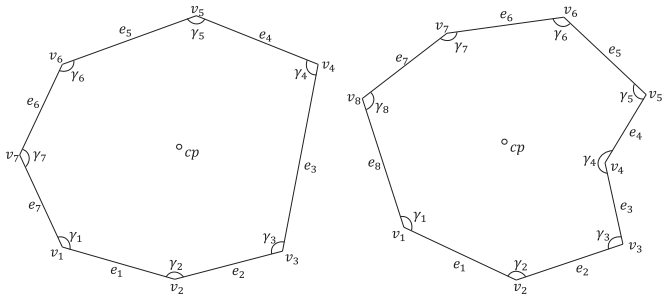

Fig. 1. Example of areas with its vertices, edges and angles. (a) Convex area. (b) Concave area.

III. E-Spiral Pattern

The area of interest is modeled as a polygon described by an ordered set of p vertices $\{v_1, \ldots, v_p\}$. Each vertex v_i is represented by a pair of coordinates $(v_x(i), v_y(i))$ and its inner angle, denoted by γ_i. For each vertex v_i, the next vertex of the polygon in the considered order is denoted by $v_{next(i)}$, where $next(i) = i(\text{mod } p) + 1$. The edge between a pair of consecutive vertices v_i and $v_{next(i)}$ is denoted by e_i, and its length by $l_i = ||v_i - v_{next(i)}||$, as illustrated in Fig. 1. We assume that the area of interest can be convex ($\forall i, \gamma_i < \pi$) or concave ($\forall i, \gamma_i > \pi$).

Given a polygonal area $A = \{v_1, \ldots, v_p\}$, the centroid point cp is computed based on the vertices. Then, the minimum distance d_{cp} from the centroid point cp to the edges e_i is calculated. The distance d_{cp}, the horizontal overlapping rate ov_x and the vertical overlapping rate ov_y are employed to calculate the number of internal layers, called rings. This procedure is crucial to determine the correct number of rings and the distance between the rings that allow to cover the entire area with the necessary overlapping required by the application. Other methods [12] in the literature do not specify an overlapping rate for the pictures and just consider the image resolution to space out the layers.

The main idea of the E-Spiral algorithm is to build a coverage path that passes by the vertices of the area of interest and decreases the radius towards the center through internal rings, as illustrated in Fig. 2. The first ring is illustrated by the gray color and starts near v_i. The distance between the rings is set as $d_r = L_x - ov_x$ and the number of rings n_r along the distance d_{cp} is computed as

$$n_r = \left\lceil \frac{d_{cp} - ov_x}{d_r} \right\rceil. \tag{1}$$

Once n_r is rounded up, we should recompute ov_x and d_r as follows:

$$\hat{ov}_x = \frac{n_r L_x - d_{cp}}{n_r - 1}, \; \hat{d_r} = \frac{d_{cp} - L_x}{n_r - 1}. \tag{2}$$

The distance d_w between consecutive waypoints in a straight line is set as $d_w = L_y - ov_y$. The number of waypoints n_w along a straight path of length $d = l_i$ is computed as

$$n_w = \left\lceil \frac{d - ov_y}{d_w} \right\rceil. \tag{3}$$

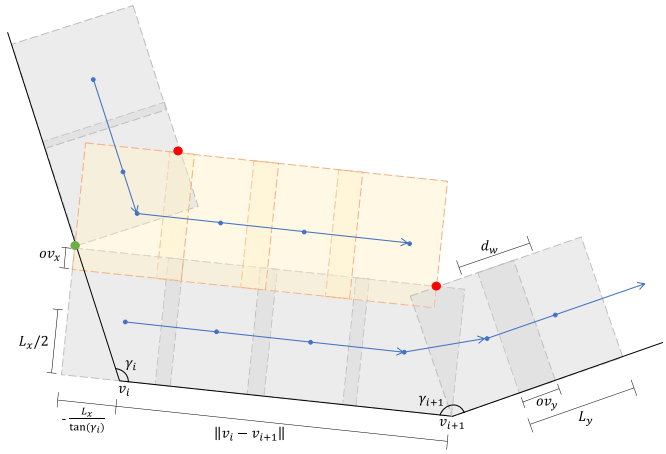

Fig. 2. E-Spiral pattern with rings, turn angles and overlapping rates.

Note that, an additional part $max(0, -L_x/tan(\gamma_i))$ is added to d only at the beginning of the path in order to connect the final part of the first ring with the beginning of the second ring, marked as a green circle in Fig. 2.

Since we have different distances between each pair of consecutive vertices, we apply different overlapping rates at each straight line, respecting the minimum value defined by the mission. Also, once n_w is rounded up, we can increase the overlap at the value $\hat{ov}_y$ such that $n_w(L_y - \hat{ov}_y) + \hat{ov}_y$ becomes exactly equal to d. That is

$$\hat{ov}_y = \frac{n_w L_y - d}{n_w - 1}. \tag{4}$$

In this way, the distance between two waypoints becomes

$$\hat{d_w} = \frac{d - L_y}{n_w - 1}. \tag{5}$$

Recomputing the overlap based on the number of waypoints will lead to an increased overlapping rate that will better allow identifying common points between each image of a set of consecutive pictures without increasing the number of rings, and hence, the traveled distance.

At each straight line, we mark the intersection points between the projected area of the last picture in the previous line and the projected area of the first picture in the current line, represented as red circles in Fig. 2. After completing a cover ring, the intersection points are set as the new vertices of the area of interest and the coverage continues in the next ring, illustrated by the orange color. Finally, we set the speed to the optimal value in every straight line of length d in order to reduce the total energy consumption of the coverage path.

The path generation procedure is summarized in Algorithm 1.

IV. Optimal Speed and Energy Estimation

The energy cost prediction of a given path is fundamental for accurate and safe coverage path planning operations. A wrong estimation may lead to unexpected crashes, while a too simplistic one may underuse the full potential of the battery, decreasing the task performance. In [1], Di Franco and Buttazzo divided

Algorithm 1: E-Spiral Algorithm.

Input: A set of vertices $\{v_1, \dots v_p\}$
Output: A set of waypoints $\{w_1, \dots w_p\}$

```
Compute the cp of the polygon specified by A
Calculate the d_cp from cp to the borders of the area
Compute n_r by (1)
Compute ô_vx and d̂_r by (2)
for j = 1 to n_r do
  for i = 1 to p do
    Compute the distance d_i and the turn angle γ_i
    Compute n_w by (3)
    Compute ô_vy and d̂_w by (4) and (5),
    respectively
    Rotate and place the first waypoint at a distance
    (L_x/2, L_y/2) from v_i and all other n_w − 1
    waypoints at a distance d̂_w from each other
  end for
  Calculate the intersection points of the projected areas
  of ring_j
  Update the vertices with the intersection points
  reducing the area
end for
Go from the final point to v_1 through a straight line
```

a generic UAV flight in simple basic measurable maneuvers, i.e., climb/descend, accelerate/decelerate, fly at constant speed, and rotate. They measured the power consumed during such operations and built an energy model upon them.

The relationship between speed and power is well known in the literature [18]. The model proposed by Di Franco and Buttazzo [1] is treated as a black box and, thanks to the real measurements, also considers external forces such as the drag of the vehicle thus making the energy model more accurate. In particular, it is possible both to estimate the energy cost of a path (splitting it into multiple straight lines) and also to find the optimal speed that minimizes such amount of energy.

In [1] the authors exploit the energy model to compute the integral of the energy for a given distance d in order to find the optimal speed that minimizes the energy necessary to travel that portion of the path. This optimal speed exists due to the total drag force curve, which combines the parasite drag and the induced drag. As the speed increases during steady flights, the parasite drag increases while the induced drag decreases [18]. This behavior leads to a minimum value for the drag curve, where the optimal speed requires less power to perform the flight, consequently saving energy. The energy model can also be used to estimate a generic path. Given m waypoints, it is possible to estimate the energy (and time) of the path as follows:

$$
\begin{aligned}
E_{path} &= E_{climb}(0,h) + E_{desc}(h,0) \\
&+ \sum_{i=0}^{m} \left(E_{acc}(0, v_i^*) + E_v(d_i, v_i^*) + E_{dec}(v_i^*, 0) \right) \\
&+ \sum_{i=0}^{m} E_{turn}(\gamma^{\{i\}})
\end{aligned} \tag{6}
$$

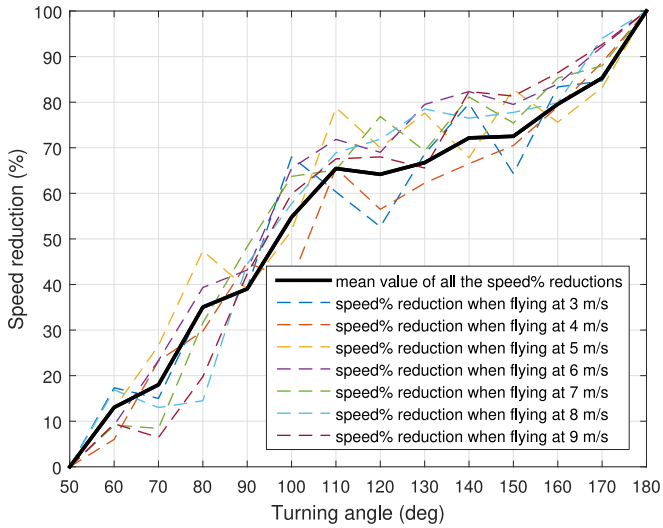

Fig. 3. Entrance speed as a function of the turning angle.

where $E_{climb}/E_{descend}$ computes the energy for climbing/descending to/from an altitude h, the first summation splits a straight line in three different phases (acceleration, deceleration, and constant speed) where v_i^* can be constant or be set to an optimal value that minimizes the straight distance for that line. Finally, the second summation takes into account the energy required for performing a rotation. All these components are pre-calculated and stored in a look-up table to speed up the computational time of the energy estimation.

A. *Optimal Speed for Spiral Paths*

The energy model proposed by Di Franco and Buttazzo presents an accurate energy estimation considering back-and-forth paths [1]. In this scenario, the model considers that the UAV starts from zero speed, reaches and keeps a constant speed, and then decelerates until zero before the turning maneuver at the end of each straight line. Thus, the energy model needs to be improved in order to deal with more complex maneuvers such as the ones performed during spiral paths, where the UAV decelerates until a given speed different from zero, performs the turn while moving, and then accelerates again.

A set of experiments were conducted to evaluate the speed variation when performing turning maneuvers from 60° to 180° at different speeds. Results obtained from real flights showed that the UAV decreases its speed according to a certain percentage when entering a curve with a specific angle as shown in Fig. 3. The figure illustrates the speed reduction percentage as a function of the turning angle, given the different initial speeds. The dashed colored lines represent the percentage reduction when performing a turn given an initial speed, while the solid black line represents the mean value for each angle.

Note that this information can be extracted by analyzing the UAV controller, but depends on the firmware/model version of the vehicle. Observing the UAV behavior through real experiments, it is possible to improve the energy model, maintaining it as a black-box independently of the controller. The same

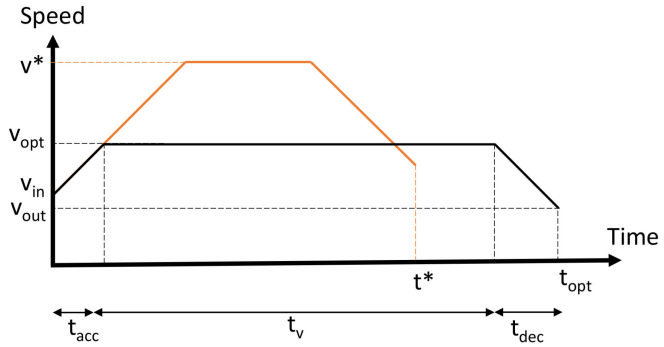

Fig. 4. The time needed to travel a straight distance can be split into three components. During t_{acc}, the quadrotor accelerates from v_{in} to a final v. Then, during t_v it flies at a constant speed and during t_{dec} it decelerates until v_{out}, that is computed considering v and the rotation angle. The optimal speed can be computed using (7).

experimental procedures can be performed on different vehicles and controllers, requiring only an initial data gathering. Knowing the entrance speed of the vehicle when it performs a given angle allows us to modify the energy model when performing the integrals for the acceleration/deceleration/constant-speed phases. The optimal speed can be computed as follows:

$$E_d(v,d,\gamma) = \int_{v_{in}}^{v} P_{acc}(v)dv + \int_{0}^{t(v)} P(v)dt + \int_{v}^{v_{out}} P_{dec}(v)dv \tag{7}$$

where $v_{out} = f(v,\gamma)$ is the entrance speed when performing the next turn with angle γ. The function $f(v,\gamma)$ is a look-up table based on the data showed in Fig. 3.

Given an initial speed v_{in}, the traveled distance d, and the turning angle γ, the energy model is able to estimate the optimal speed v and the amount of energy E_d required to fly the traveled distance d. Fig. 4 shows a graphical illustration of the modified equations. The distance d can be covered at different speeds, leading to different travel times. However, we are interested in minimizing the energy, not the time, since a shorter time may require a larger amount of energy depending on the circumstances. Differently from the original energy model, v_{in} and v_{out} depend on the specific path and are not always zero.

V. Experimental Results

In this section, we validate the two main contributions of the work through simulations and real experiments. First, we compare the E-Spiral algorithm with respect to the E-BF in simulations over several different areas of interest. Then, we show the results performed on real flight experiments with both algorithms in two different scenarios in order to measure the energy spent during the missions. Finally, we show the results of a test performed to verify the accuracy of the improved energy model comparing the real energy with respect to the estimated one. We remark that predicting the cost of a path is crucial to avoid unexpected crashes and make an efficient use of the battery capacity.

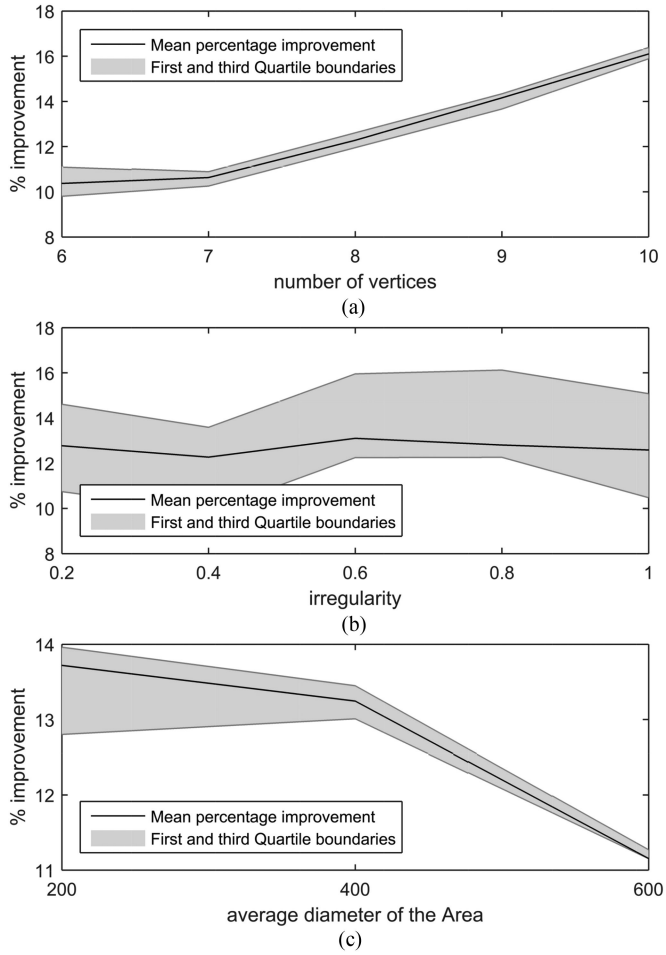

Fig. 5. Percentage improvement of the E-Spiral over the E-BF varying (a) the number of vertices, (b) levels of irregularity, (c) the size of the areas of interest. In all the cases E-Spiral outperforms E-BF.

A. MATLAB Simulations

The algorithms have been implemented on MATLAB. A wide range of simulations were performed over a set of polygonal areas of interest with different characteristics, such as the number of vertices (varying from 6 to 10), the levels of irregularity (varying from 0 to 1 and indicating the variance in the angular spacing of vertices), and the size of the area (average diameter from 200 to 600 meters). For each setting (number of vertices, irregularity, area), 50 different areas were generated, with a total number of 3750 tested areas.

Fig. 5 presents the percentage of improvement of the E-Spiral over the E-BF algorithm considering several areas of interest with different characteristics. The benefits of the E-Spiral increases with the number of vertices of the area, as illustrated in Fig. 5(a). This was expected, since the E-BF works better with simple and long areas. The different levels of irregularity impact equally both algorithms and the average improvement is constant around 13%, as shown in Fig. (b). Finally, the performance of E-Spiral decreases as the area increases, as shown in Fig. (c). This was also expected, since the E-BF will benefit from longer straight distances, and the effect of turns is less relevant.

(a) (b) (c) (d)

Fig. 6. Real flight paths generated with E-Spiral and E-BF algorithms for rectangular and polygonal areas. (a) E-Spiral algorithm in polygonal area. (b) E-BF algorithm in polygonal area. (c) E-Spiral algorithm in rectangular area. (d) E-BF algorithm in rectangular area.

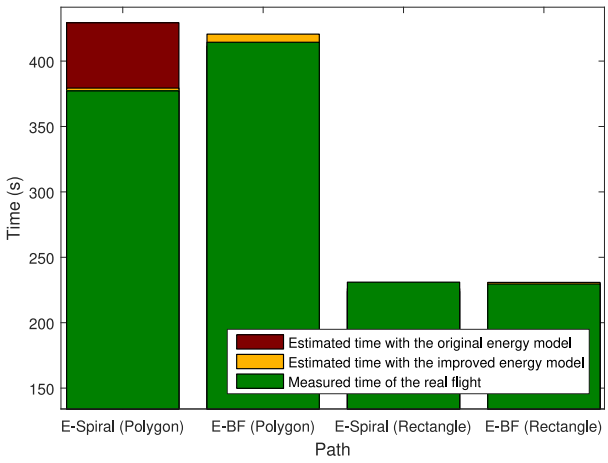

Fig. 7. Mission execution time for simulation and real flights with E-Spiral and E-BF algorithms in rectangular and polygonal areas. The accuracy of the mission time estimation varies from 96.93% to 99.47%.

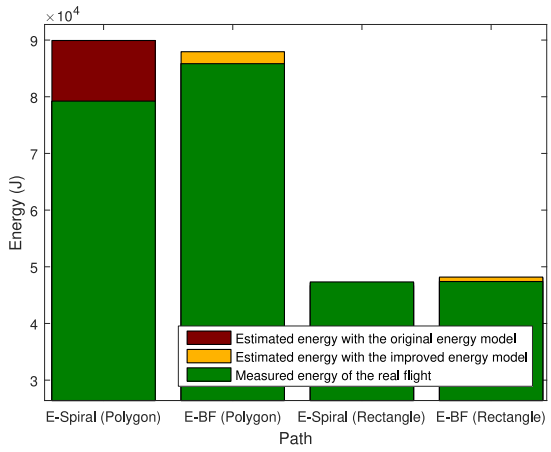

Fig. 8. Energy consumption for simulation and real flights with E-Spiral and E-BF algorithms in rectangular and polygonal areas. The accuracy of the energy estimation varies from 97.54% to 99.91%.

B. Real Flights

In the real flight experiments, we used an IRIS quadrotor with a GoPro camera mounted on a Gimbal stabilizer. The quadrotor weighs about 1.3 Kg and carries a LIPO 3 S battery. The autopilot is an Arducopter 3.2 on top of a PixHawk board. For each flight, the autopilot saves a log with all the useful information to analyze the experiment (GPS, speed, altitude, voltage, and current, etc.).

Our setup is composed of two different areas of interest: a polygon and a rectangle. The two areas have been chosen to highlight the differences between the two algorithms. In particular, the E-Spiral may be more effective when used in a polygon area while the E-BF should benefit from a rectangular area. Moreover, while the improved energy model will behave similarly to the original in the rectangular area due to 90° turns, a difference between the two should be evident when estimating the energy consumption of the polygon area paths. Fig. 6 illustrates the areas of interest (red), the planned path (blue), the performed path during the real flights (white), the starting position (green "x"), and the final position (red "x").

The results of the experiments can be seen in Figs. 7 and 8. The green bars represent the results from the flights performed with paths generated by the E-Spiral algorithm and the E-BF algorithm. The red and the yellow bars illustrate the estimation values for the energy consumption and the mission execution time, obtained through the energy model previously proposed by [1] and improved in this letter, respectively. Experimental results show that E-Spiral algorithm overcomes E-BF in both areas of interest, reducing the mission execution time around 9% and the energy consumption around 7.7%, stating the effectiveness of the proposed approach.

TABLE I
MISSION EXECUTION TIME AND ENERGY CONSUMPTION IN SIMULATION AND REAL FLIGHTS WITH THE E-SPIRAL AND THE E-BF IN POLYGONAL (P) AND RECTANGULAR (R) AREAS

Path	Real	Estimated	Prev. Estimated	Accuracy
E-Spiral (P)	377.2 s	379.35 s	429.29 s	99.43%
E-BF (P)	414.4 s	420.60 s	411.43 s	98.50%
E-Spiral (R)	231.0 s	223.91 s	226.04 s	96.93%
E-BF (R)	229.6 s	230.81 s	230.26 s	99.47%
E-Spiral (P)	79228J	79158J	89924J	99.91%
E-BF (P)	85837J	87945J	85845J	97.54%
E-Spiral (R)	47329J	46681J	47143J	98.63%
E-BF (R)	47401J	48182J	48030J	98.35%

Table I presents detailed information about the time and the energy results comparing the E-Spiral and the E-BF algorithms using different areas of interest. The flight results also stated the

high precision rate of the improved energy model employed as an estimation energy tool. Using the (7), it is possible to correctly estimate the energy needed to perform a certain path splitting it into simple maneuvers as climbing, descending, turning, accelerating/decelerating and flying at constant speed. The accuracy rate between the simulation and the real flights regarding the mission execution time varies from 96.93% to 99.47%, while the energy accuracy varies from 97.54% to 99.91%, approximately. In this way, we are able to avoid crashes during flights due to battery-exhaustion. Moreover, it is important to highlight that the improved energy model increases the time and the energy estimation precision of 13.24% and 13.41%, respectively.

VI. Conclusion

In this letter, we proposed a novel Energy-aware Spiral Coverage Path Planning algorithm for photogrammetric applications. The algorithm generates paths considering overlapping rates and uses the camera characteristics as image resolution and field of view to guarantee a complete area mapping. The algorithm also uses an energy model to set different optimal speeds for each straight segment of the path to save energy. We compared the proposed approach with the E-BF, a previously proposed energy-aware back-and-forth algorithm, through a wide range of simulations considering areas of interest with different characteristics, such as the number of vertices, the irregularity, and the size of the area. Results showed that E-Spiral outperforms E-BF in all the cases, providing an effective energy saving even in the worst scenario (large areas and few vertices) with a percentage improvement of 10.37% up to the best case (high number of vertices) with 16.1% of improvement. Real flights were also performed in rectangular and polygonal areas. E-Spiral overcomes E-BF in both areas reducing the time around 9% and the energy around 7.7%, stating the effectiveness of the proposed approach.

We also proposed an improvement for the energy model to predict the overall energy cost in spiral paths, considering the entrance speed and the turning angle in order to obtain an even more precise system. The modified energy model showed an improvement in the estimation precision of time and energy up to 13.24% and 13.41%, respectively.

As a future work, we intend to explore the effect of wind fields during the coverage missions in order to generate energy-efficient trajectories through energy maps. Further investigations are also necessary to explore the energy model as a generic estimation tool for comparing any CPP algorithm.

References

[1] C. Di Franco and G. Buttazzo, "Coverage path planning for UAVs photogrammetry with energy and resolution constraints," *J. Intell. Robot. Syst.*, vol. 83, no. 3–4, pp. 445–462, 2016.

[2] C. Nattero, C. T. Recchiuto, A. Sgorbissa, and F. Wanderlingh, "Coverage algorithms for search and rescue with UAV drones," in *Proc. XIII AI*IA Symp. Artif. Intell. Workshop*, Dec. 2014.

[3] A. Barrientos *et al.*, "Aerial remote sensing in agriculture: A practical approach to area coverage and path planning for fleets of mini aerial robots," *J. Field Robot.*, vol. 28, no. 5, pp. 667–689, Sep. 2011.

[4] D. W. Casbeer, D. B. Kingston, R. W. Beard, and T. W. McLain, "Cooperative forest fire surveillance using a team of small unmanned air vehicles," *Int. J. Syst. Sci.*, vol. 37, no. 6, pp. 351–360, 2006.

[5] A. Stalmakou, "UAV/UAS path planning for ice management information gathering," Master's thesis, Dept. Eng. Cybern., Norwegian Univ. Sci. Technol., Norway, 2011.

[6] C. Castiblanco, J. Rodriguez, I. Mondragon, C. Parra, and J. Colorado, *Air Drones for Explosive Landmines Detection*. New York, NY, USA: Springer, 2014, pp. 107–114.

[7] C. Liu, Y. Liu, H. Wu, and R. Dong, "A safe flight approach of the UAV in the electrical line inspection," *Int. J. Emerg. Elect. Power Syst.*, vol. 16, no. 5, pp. 503–515, 2015.

[8] M. Aghaei, P. Bellezza Quater, F. Grimaccia, S. Leva, E. Ogliari, and M. Mussetta, "Pv plant planning and performance monitoring by means of unmanned aerial systems (UAS)," in *Proc. 8th AIGE (Italian Association of Energy Management) Nat. Conf.*, Jun. 2014, pp. 55–60.

[9] H. Choset, "Coverage for robotics – A survey of recent results," *Annals Math. Artif. Intell.*, vol. 31, no. 1, pp. 113–126, 2001.

[10] H. L. Andersen, "Path planning for search and rescue mission using multicopters," Master's thesis, Dept. Eng. Cybern., Norwegian Univ. Sci. Technol., Norway, 2014.

[11] M. Oborne, Mission planner - ground station. [Online]. Available: http://planner.ardupilot.com, Accessed on Jun. 15, 2017.

[12] G. Öst, "Search path generation with UAV applications using approximate convex decomposition," Master's thesis, Dept. Elect. Eng., Sweden, Linköping University, 2012.

[13] Y. Li, H. Chen, M. J. Er, and X. Wang, "Coverage path planning for UAVs based on enhanced exact cellular decomposition method," *Mechatronics*, vol. 21, no. 5, pp. 876–885, 2011.

[14] M. Torres, D. A. Pelta, J. L. Verdegay, and J. C. Torres, "Coverage path planning with unmanned aerial vehicles for 3D terrain reconstruction," *Expert Syst. Appl.*, vol. 55, pp. 441–451, 2016.

[15] "Quasi-greedy triangulations approximating the minimum weight triangulation," *J. Algorithms*, vol. 27, no. 2, pp. 303–338, 1998.

[16] J. W. Langelaan *et al.*, "Green flight challenge: Aircraft design and flight planning for extreme fuel efficiency," *J. Aircr.*, vol. 50, no. 3, pp. 832–846, 2013.

[17] A. Chakrabarty and J. W. Langelaan, "Energy-based long-range path planning for soaring-capable unmanned aerial vehicles," *J. Guid., Control, Dyn.*, vol. 34, no. 4, pp. 1002–1015, 2011.

[18] W. Johnson, *Rotorcraft Aeromechanics*. Cambridge, U.K.: Cambridge Univ. Press, 2013, vol. 36.